

Removal of brilliant green from aqueous solution by *Pyrus pashia* leaves powder as an adsorbent: equilibrium, thermodynamic and kinetics studies

Rashida Fiaz^a, Muhammad Hafeez^{a,*}, Mahmood Rashid^a, Abrar Niaz^b, Azeem Bibi^a

^aDepartment of Chemistry, University of Azad, Jammu & Kashmir, Muzaffarabad, Pakistan, emails: smhafeezkhan@yahoo.com (M. Hafeez), abrarashida@gmail.com (R. Fiaz), rashid_meh786@yahoo.com (M. Rashid), azeembibi786@gmail.com (A. Bibi)

^bInstitute of Geology, University of Azad, Jammu & Kashmir, Muzaffarabad, Pakistan, email: abrar.niaz@ajku.edu.pk

Received 9 August 2020; Accepted 9 January 2021

ABSTRACT

The dyes used in textile industries are very toxic and harmful compounds and they have a very negative effect on the environment, especially when they are discharged into soil and water. In a recent study, the very cost-effective and abundantly available biomass sorbent *Pyrus pashia* leaves was employed for the removal of brilliant green from wastewater. Several variables like initial dye concentration (10–50 mg/L), contact time (10–70 min), the dosage of *Pyrus pashia* leaves (0.15–0.45 g), pH (3–14), temperature (25°C–50°C) and desorption studies were performed for the investigation of the batch experiment. The maximum brilliant green removal was obtained to be 93.35% at optimized experimental conditions. The equilibrium data were described by different adsorption isotherm models (Langmuir, Freundlich and Temkin). The results showed that the experimental data were best fitted with the Langmuir isotherm model with $R^2 = 0.99$ which describes the monolayer formation of brilliant green on the *Pyrus pashia* leaves outer surface. The adsorption kinetics models (pseudo-first-order, pseudo-second-order and Elovich model) were also applied and experimental data best followed the pseudo-second-order kinetics model with $R^2 > 0.98$. The thermodynamic parameters such as ΔH° , ΔG° and ΔS° were also calculated. The physical properties were also examined by using Brunauer–Emmett–Teller and the surface morphology of the adsorbent was studied by scanning electron microscope. The experimental results showed that the adsorbent *Pyrus pashia* leaves can be effectively used for the brilliant green removal from the wastewater.

Keywords: *Pyrus pashia*; Brilliant green; Removal efficiency; Adsorption capacity

1. Introduction

Nowadays, rapid industrial development gave a big impression on environmental society. The textile industries have the highest contribution to dyes utilization for fiber coloration. The textile effluents contain a large amount of dyes along with different additives during the whole coloring process [1]. The colored effluents discharged from industries are considered to be less harmful and toxic than many colorless effluents. These are presented by the public on the ground that color is an indicator of pollution [2].

Due to color, dyes are the most easily identifiable pollutants. Therefore, people must be familiar with the concentration of dye used in mineral water because it can cause severe health problems to human beings. The dyes stuff production of different types now reaches 700,000–100,000 tons annually. Dyes are divided into two categories as cationic and anionic on the basis of their structure [3–6]. The dyes must be eliminated before their release into the environment. For this reason, tight restrictions on the organic contents must be followed. The dyes have toxic and carcinogenic behavior when discharged into water. Most of the dyes are

* Corresponding author.

This article was originally published with an error in the names of the first two authors. This version has been corrected. Please see Corrigendum in vol. 221 (2021) 447 [10.5004/dwt.2021.27421].

carcinogenic and toxic when discharged into the water and they cause serious damage to aquatic life. There are many techniques employed for the dye removal from wastewater such as ultrafiltration, flocculation and coagulation, electrochemical degradation, and ion-exchange method and adsorption. The researchers showed that adsorption is the best and convenient technique and has given better results in different coloring materials from the wastewater. Adsorption is considered to be a potential method for dye removal from industrial wastewater [7,8]. The activated carbon is also applied for adsorption of dye removal prepared from milk vetch, malachite green by nanoparticle of zinc oxide, adsorption of bisphenol A prepared from synthetic carbon and natural material, bromophenol blue and nanoparticle loaded zinc sulfide for brilliant green (BG) removal [9–13]. Therefore, many studies, showed that biomass or natural materials are the best alternative adsorbents due to reliable resources, low-cost and environment-friendly instead of activated carbon (commercial) adsorbent [14–16]. The adsorbent has adsorbing material which has many elements that can remove pollutant [17]. The activated carbon due to many disadvantages such as it is costly, ineffective and nonselective against vat and disperses dyes is not widely used [18]. So many economic and easily available adsorbents for the treatment of synthetic dyes are introduced in recent years and has attracted great interest to prevent the water from pollution caused by dyes and protect the environment. Fiaz et al. [45] also introduced low-cost biowaste adsorbents such as *Salix alba*, *Viburnum grandiflorum* and *Pyrus pashia* for dye removal with percentage removal of 95.2%, 95.59% and 98% respectively. These are easily and abundantly available biomass and environment friendly than activated carbon. Thus, the basic purpose of the recent study is also to come out with a suitable and cost-effective technique for the removal of brilliant green from wastewater. The *Pyrus pashia* leaves powder low-cost and freely available biomass has been used for the removal of BG from an aqueous solution.

2. Experimental

2.1. Solutions and reagents

The solutions used in the experimental work were prepared by using distilled water. Brilliant green was bought from BDH Chemicals (England) and was utilized without further purification. The molecular weight of the BG is 482.634 g/mol and the structure is given in Fig. 1. The stock solution of brilliant green was prepared by mixing 1 g of BG in distilled water (1,000 mL). The dilution of the dye stock solution was carried out for preparing further solutions for experimental work to attain the required concentrations of BG (10–50 mg/L). The pH of the solutions was maintained by utilizing NaOH (0.1 M) and HCl (0.1 M). The pH of the solutions was measured using a pH meter.

2.2. *Pyrus pashia* (biosorbent) preparation

The village Rairban District Bagh, Azad Jammu and Kashmir, Pakistan was selected for the collection of *Pyrus pashia* leaves. They were dipped in water for 24 h, then

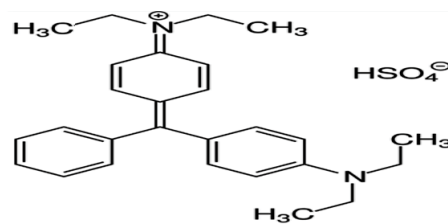


Fig. 1. Structure of BG dye.

distilled water was used for washing the leaves and placed in the open air for drying for a few days. Afterward, fine powder of leaves was obtained by grinding them with an electric grinder and sieved through 70 mesh sieves.

2.3. Characterization of *Pyrus pashia* leaves and Methylene Blue

The properties (physical and chemical) of biosorbents are necessary for the investigation of their adsorption capacities. Different techniques were employed for the characterization of *Pyrus pashia* leaves powder such as UV-Vis spectrophotometer and Fourier-transform infrared (FTIR) spectrophotometer. The exterior morphology of biosorbent powder was seen by scanning electron microscope (SEM). The thermogravimetric analysis/differential scanning calorimetry (TGA/DSC) analysis was performed by utilizing the instrument Universal V.4.5A TA, SDT Q600 V 20.9. The *Pyrus pashia* leaves powder surface area was obtained by Quantachrome NOVWin V (Quantachrome and Anton Paar Boynton Beach, Florida). 11.04. The calculated results of bulk density and moisture contents are given in Table 1.

2.4. Desorption studies

The experiments for desorption were performed in batch with different desorbing reagents such as 0.1 M KCl, NaOH, HCl and distilled water. The adsorbent (*Pyrus pashia*) 0.15 g and 50 mL of dye solution (50 mg/L) were treated for 2 h. The BG loaded biosorbent was washed by distilled water for the removal of unabsorbed dye and then shaken with various desorbing agents (25 mL). The desorbed BG concentration was determined and Eq. (1) was used for the calculation of % desorption.

$$\% \text{Desorption} = \frac{m_d}{m_a} \times 100 \quad (1)$$

where m_d (mg/L) BG desorbed amount and m_a (mg/L) represent the adsorbed BG amount, respectively.

2.5. Batch equilibrium and kinetic studies

The experiments for batch studies were performed by preparing BG solution of 50 mL using three conical flasks (250 mL each) with *Pyrus pashia* leaves (0.15 g). The mixtures were stirred and heated at different temperatures as 303, 313 and 323 K, respectively. The filtration of mixtures was carried out and filtrate absorbance was measured using UV-Vis spectrophotometer for brilliant green having λ_{max} (625 nm). The determination of equilibrium concentrations of

Table 1
Physical properties of *Pyrus pashia* leave powder

Adsorbent	Surface area, (m ² /g)	Water contents, (%)	Bulk density, (g/cm ³)
<i>Pyrus pashia</i>	220.62	2.14	0.41

the samples was carried out by applying Beer–Lambert law and Eq. (2) was employed in the calculation of adsorption capacity.

$$q_e = \frac{(C_0 - C_e)V}{m} \quad (2)$$

where m is the mass of *Pyrus pashia* leaves in (g). C_0 initial BG concentration and C_e BG concentrations at equilibrium (mg/L) and V is the volume of solution (L). The percentage removal was calculated by employing Eq. (3) [19].

$$\%R = \frac{(C_0 - C_e)}{C_0} \times 100 \quad (3)$$

The evaluation of experimental was data conducted using isotherm adsorption models (Freundlich, Langmuir and Temkin). The Langmuir equation is shown as:

$$\frac{C_e}{q_e} = \frac{1}{Q_0 b} + \left(\frac{1}{Q_0}\right) C_e \quad (4)$$

Here Q_0 designates the dye uptake capacity.

The R_L Langmuir isotherm dimensionless factor equation is shown as:

$$R_L = \frac{1}{1 + bC_0} \quad (5)$$

where BG initial concentration is shown by C_0 (mg/L). The nature of the process of adsorption can be determined by the dimensionless factor R_L of Langmuir isotherm [20]. If R_L ($0 < R_L < 1$) then favorable for adsorption process, un-favorable ($R_L > 1$), linear ($R_L = 1$) or irreversible ($R_L = 0$). The heterogeneity of the system can be determined by Freundlich [21] model using an empirical isotherm.

$$\ln q_e = \ln K_f + \frac{1}{n} \ln C_e \quad (6)$$

where K_f (mg/g (L/mg)^{1/n}) and n are constants of Freundlich isotherm in Eq. (6). The Temkin isotherm model Eq. (7) is given as:

$$q_e = B \ln A + B \ln C_e \quad (7)$$

where $RT/b = B$ which is the heat constant of adsorption, $b =$ Temkin constant of the heat of adsorption (J/mg), $T =$ absolute temperature (K) and $A =$ equilibrium constant for maximum binding energy (L/g).

The nature of the process of adsorption was studied by carrying out the thermodynamic studies, using different scientific relations like change in entropy (ΔS° , J/K mol), enthalpy change (ΔH° , kJ/mol) and free energy change (ΔG° , kJ/mol) [Eqs. (8) and (9)].

$$\Delta G = -RT \ln K_c \quad (8)$$

$$\ln K_c = \frac{-\Delta G^\circ}{RT} = -\frac{\Delta H^\circ}{RT} + \frac{\Delta S^\circ}{R} \quad (9)$$

In Eq. (9), K_c is the equilibrium constant, R (8.314 J/K mol) is the gas constant and T represents temperature in Kelvin.

3. Results and discussion

3.1. Characterization of *Pyrus pashia* leaves powder

The characterization of powder of *Pyrus pashia* leaves was performed by several techniques like FTIR. The analysis was measured between 500 and 4,000 cm⁻¹. The surface morphology was studied by scanning electron microscope. The TGA/DSC analysis of *Pyrus pashia* leaves was also done. The instrument Quantachrome NOVWin V. 11.04 was applied in the determination of *Pyrus pashia* leaves powder surface area. The results of bulk density, moisture contents and surface area are given in Table 1.

3.2. FTIR analysis

The FTIR analysis of *Pyrus pashia* leaves was performed from 4,000 to 500 cm⁻¹ by employing the FTIR spectrophotometer to examine the surface functional groups. The prominent peak at 3,401 cm⁻¹ in the IR spectrum of before adsorption was because of water on the *Pyrus pashia* leaves surface as well as stretching vibrations of amine, the peak obtained at 1,724 cm⁻¹ represents the weak combinations and overtones, aromatic C=C bonding, the 1,365 cm⁻¹ prominent peak shows ring stretching vibrations of esters, C–O stretching of alcohols, ethers and carboxylic acids present on the adsorbent surface (Fig. 2a). The peak at 1,216 cm⁻¹ is that of N–H stretching vibrations and the peak at 526 cm⁻¹ is attributed to C–S linkage. The appearance of new peaks at 2,999 and 3,602 cm⁻¹ in *Pyrus pashia* leaves adsorbent after adsorption of BG also confirm the physio-chemical interaction between adsorbate and adsorbent. The significant changes in the frequencies were observed after adsorption spectra (Fig. 2b). This figure showed that the functional group's participation in the process of adsorption was may be due to van der Waals forces, physical linkage or chemical bonding [22,23].

3.3. SEM analysis

The *Pyrus pashia* leaves powder was analyzed by SEM before and after BG adsorption (Figs. 3a and b). The difference in both the images delineated that porous surfaces (before adsorption) become smooth due to adsorption of BG onto *Pyrus pashia* leaves surfaces.

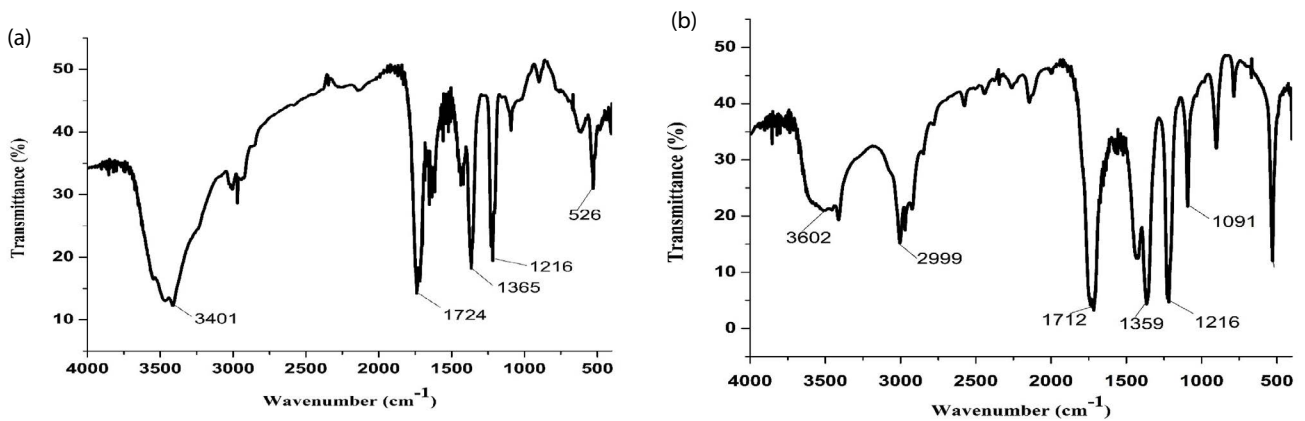


Fig. 2. IR spectrum of *Pyrus pashia* leaves (a) before adsorption and (b) after adsorption.

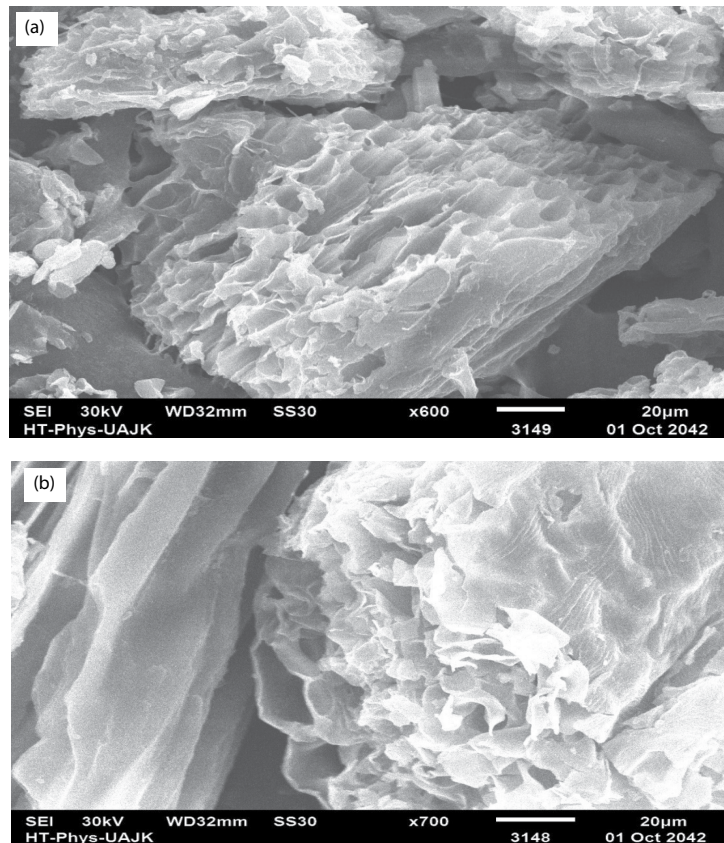


Fig. 3. BG adsorbed *Pyrus pashia* leaves SEM micrographs (a) before adsorption and (b) after adsorption.

3.4. Thermal analysis

The plot between mass loss and temperature is shown in Fig. 4. Three distinct phases are shown in TGA analysis. In the initial phase (0°C–250°C), the slow mass loss was obtained due to the evaporation of water and volatile compounds. In this phase, decomposition occurred [24]. The % mass loss at the first phase was calculated to be 20.10% and at 250°C this phase ended. The second or next phase (250°C–380°C) showed a rapid mass loss due to the roasting of the sample and the % mass loss was found to

be 41.75%. The maximum mass loss was observed for the sample which is basically due to the organic matter decomposition and biomass components containing hydroxyl groups. The third phase (380°C–789°C), shows the percent mass loss of 18.12% due to the solid-residue decomposition [25,26]. According to differential scanning calorimetric analysis, two main phases were observed, the first negative peak represented the endothermic phase (below 100°C) which is due to the evaporation of moisture contents and different volatile compounds (Fig. 4).

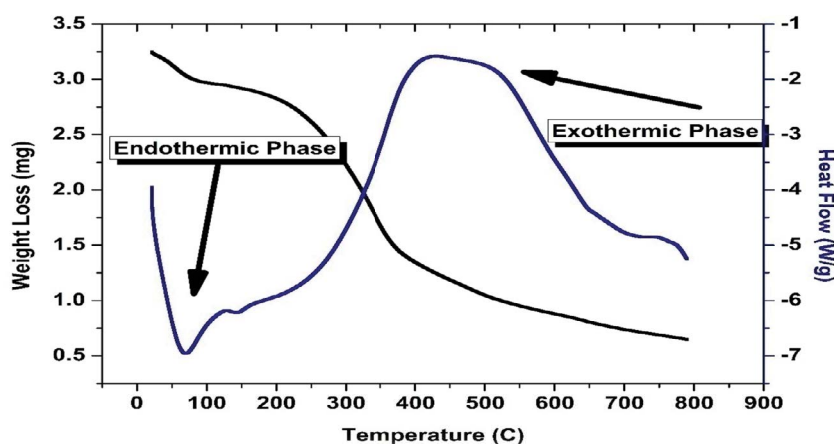


Fig. 4. A graph of TGA/DSC analysis.

The positive peak above 100°C was observed which represented an exothermic phase indicating the decomposition of cellulose, hemicelluloses and lignin [27].

3.5. Contact time effect

The contact time variations between dye (BG) and adsorbent (*Pyrus pashia* leaves) are beneficial in studying the volume of adsorbed dye at varying time intervals at fixed biosorbent dosage. The equilibrium time is very important in the wastewater treatment process. This effect was studied by varying the contact time from 10–70 min, the concentration of BG (50 mg/L), biosorbent dosage (0.15 g) and pH (5) at 298 K. The dye uptake (1.407–15.55 mg/g) and removal efficiency (93.35%) increased from 10–70 min, while equilibrium was obtained at 50 min. The adsorption of the dye was rapid at the initial stages of the adsorption and equilibrium was obtained within 50 min. It is due to permeation on an adsorbent surface (because of accretion of adsorption positions by the ions of dye) whole surface area of adsorbent and more diffusion rate reduced at prolonged contact time. The value of maximum percentage removal was obtained at 50 min with a slight increase up to 70 min. This is because of the presence of excessively exposed adsorption sites are present which accelerate the adsorption rate due to diffusion towards sites of adsorbent (*Pyrus pashia* leaves) from the BG solution [28,29]. The comparison of dye uptake capacities for various adsorbents are presented in Table 5.

3.6. Effect of preliminary dye concentration

The concentration of the adsorbate solution greatly affects the process of adsorption because the reactions of adsorption are directly related to the solute concentration. The preliminary concentration of dye affects the adsorption capacity. This parameter was studied by taking 10–50 mg/L initial BG concentration at 50 min time of equilibrium and pH = 5 at temperature (298 K). Fig. 5 shows that the increase in dye uptake capacity (1.407–15.55 mg/g) was observed with an initial concentration of BG (10–50 mg/L). The removal of dye from wastewater by the process of adsorption depends primarily on mass

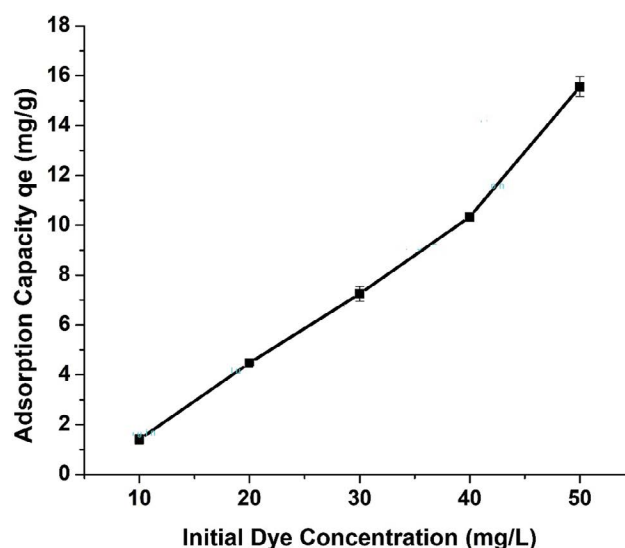


Fig. 5. Effect of dye concentration on BG adsorption using *Pyrus pashia* leaves (contact time 50 min; pH = 5; temperature 298 K).

transfer for the initial dye concentration. So at a higher concentration of dye, the adsorption capacity increased by the driving force responsible for mass transfer [30].

3.7. Biosorbent dosage effect

The adsorbent dosage also affects BG adsorption onto *Pyrus pashia* leaves. The fixed dye initial concentration was employed in the determination of the adsorption capacity of an adsorbent. The adsorbent dosage effect was studied for the BG removal by *Pyrus pashia* leaves. The results showed (Fig. 6) that the percentage removal increases with an increase in biosorbent dose (0.15–0.45 g) and the maximum percent removal (93.22%) was obtained at 0.45 mg/g. The adsorption capacity (mg/g) decreases from 10.41 to 4.09 mg/g with an increase in adsorbent dosage (0.15–0.45 g). The decrease was due to remaining unsaturated active sites on the surface of adsorbent for the adsorption of dye [31].

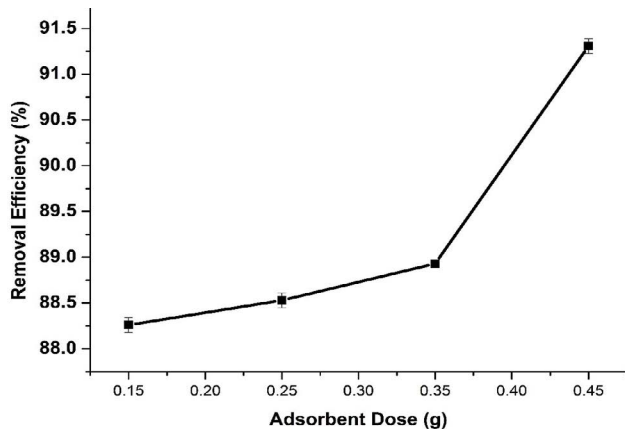


Fig. 6. BG loaded *Pyrus pashia* leaves plot of percentage removal vs. adsorbent dose.

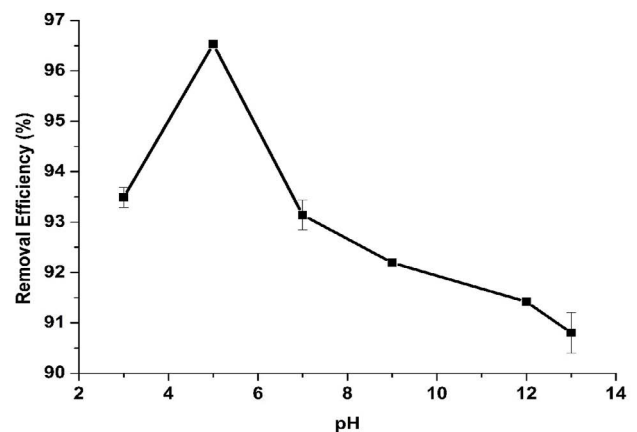


Fig. 7. BG loaded *Pyrus pashia* leaves plot of percentage removal vs. pH.

3.8. Effect of pH

The most significant parameter in the adsorption studies is the solution pH, which affects the charge on the adsorbent surface, degree of the molecule of dye (adsorbate) ionization, and the degree of functional groups detachment on the active sites present on adsorbent. The percentage removal of *Pyrus pashia* leaves is influenced by the pH of the BG solution (Fig. 7). The maximum (96.53%) removal efficiency was observed with 50 mg/L initial BG concentration at pH = 5 with 50 min equilibrium time. The increase in pH also enhanced removal efficiency. The repulsive electrostatic forces have been generated by positive charges on the *Pyrus pashia* leaves surface which makes the adsorption process unfavorable [32,33]. The dye molecule's competition with protons at adsorbent active sites having acidic pH are responsible for the low dye uptake capacity [34]. The electrostatic attraction due to negative charges on the *Pyrus pashia* leaves surface enhanced the adsorption process. So the adsorption capacity (12.87 mg/g) was obtained at pH = 5 and then declined up to pH = 13. The zero point charge (pH_{zpc}) can be used to explain the pH effect on the percentage removal of BG. When the pH of the solution is below pH_{zpc} then the surface of the adsorbent becomes positively charged. Whereas the adsorbent surface becomes negatively charged when the pH of the solution is above the pH_{zpc} . In the present study, the maximum removal efficiency was obtained at pH = 5. The study showed that the cationic sites of functional groups are more than ionic sites in acidic medium, due to which there is a chelate formation with basic dye ions. More OH^- ions in basic pH hinder the anionic dye adsorption due to repulsive forces.

3.9. Effect of temperature

The temperature effect was studied by taking 0.15 g *Pyrus pashia* leaves dosage and equilibrium time of 50 min with 50 mg/L initial BG concentration at pH = 5. The variation of temperature (298–323 K) is shown in Fig. 8. The enhancement of removal percentage and dye uptake capacity with temperature delineated the endothermic nature of the process [25]. The high temperature enhances

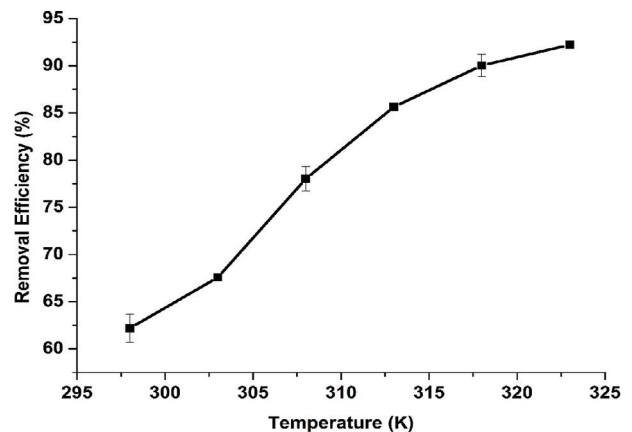


Fig. 8. The percentage removal plot of BG loaded *Pyrus pashia* leaves at variable temperatures.

dye molecules' movements hence dye molecules and the surface functional groups reaction activated at elevated temperatures [35].

3.10. Adsorption thermodynamics

The characterization of the adsorption process was carried out by thermodynamic studies like entropy change (ΔS°), change in free energy (ΔG°) and enthalpy change (ΔH°). The graph between $1/T$ vs. $\ln K$ was employed in the ΔS° and ΔH° values calculation. The positive ΔH° (60.018) is the indication of an endothermic reaction for the BG loaded *Pyrus pashia* leaves adsorption. The spontaneity and feasibility of the reaction are also depicted by negative values of ΔG° in Table 2. The positive ΔS° (249.66) shows an attraction of *Pyrus pashia* leaves for BG and also shows increased randomness at the solid-solution interface (Fig. 9).

3.11. Equilibrium studies

The equilibrium isotherms have been employed for the description of adsorbate (dye) taken up by the adsorbent

Table 2
BG loaded *Pyrus pashia* leaves results for the thermodynamic study

Temperature (K)	ΔG (kJ/mol)	ΔH (kJ/mol)	ΔS (kJ/mol)
303	-16.44		
313	-19.75	60.018	249.66
323	-22.15		

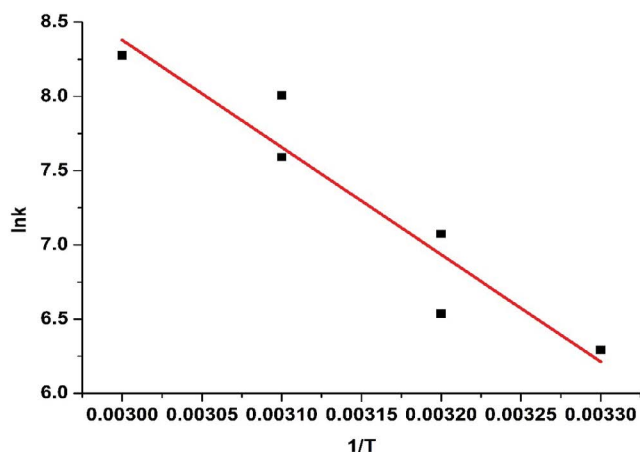


Fig. 9. The plot of adsorption thermodynamics for BG adsorbed *Pyrus pashia* leaves.

(biomass) concentration that remained in a solution. The different equations were applied to the equilibrium data measured in the adsorption process. The models depict information related to the adsorption mechanism, adsorption capability as well as surface properties of the adsorbent. The study shows the calculation of *Pyrus pashia* leaves q_e (dye uptake capacity) using isotherm models (Temkin, Langmuir and Freundlich) from aqueous solution for percent BG removal [36]. The isotherms adsorption at 303, 313 and 323 K were carried for BG loaded *Pyrus pashia* leaves. The Langmuir model is more applicable for an explanation of the homogeneity of the adsorption sites. The different monolayer adsorption studies have been carried out using this model [37]. It was investigated that BG loaded *Pyrus pashia* leaves best constraints with the Langmuir isotherm. Hence, C_e vs. C_e/q_e (Fig. 10) is a straight-line plot having $(1/Q_e b)$ an intercept and $(1/Q_e)$ slope (Table 3). The Langmuir isotherm presents adsorbent surface homogeneity. The development of equivalent small patches of energy levels on the adsorbent surface has been observed during the process of adsorption [38]. The R^2 (correlation coefficient) values (0.9957) are showing best match with Langmuir isotherm. The R^2 value delineated that the adsorption data for BG loaded *Pyrus pashia* leaves best matches the Langmuir isotherm. The maximum adsorption capacity at higher temperatures showed that the BG adsorption onto *Pyrus pashia* leaves is the chemisorption process in which the chemical interactions are involved between adsorbent and adsorbate.

Moreover, the Freundlich model is applicable to the non-ideal or heterogeneous adsorption. This model constraint

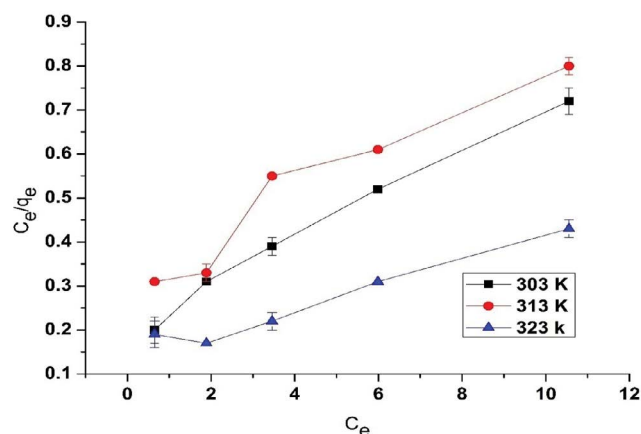


Fig. 10. BG loaded *Pyrus pashia* leaves results of the Langmuir isotherm model at varying temperatures.

with a multilayer system of adsorption [37,38]. The plot of straight-line (Fig. 11) was drawn between $\ln q_e$ and $\ln C_e$ showing $\ln K$ (intercept) and $1/n$ is (slope). The *Pyrus pashia* leaves adsorption parameters have been narrated in Table 3 [39]. The data obtained by experiments were also applied to the Temkin isotherm model (Fig. 12). This model describes that a decline in the heat of adsorption is linear and that the adsorption is described by a uniform binding energy distribution. The linear form of the Temkin model is represented in Eq. (7). The Temkin constants are shown in Table 3.

3.12. Adsorption kinetics

The adsorption kinetics study can explain the adsorption mechanism and the rate of the adsorption process. The dye adsorption on the adsorbent (solid) surface can be explained by two different mechanisms initially the fast binding of adsorbate molecules on the biosorbent surface and then the slow intraparticle diffusion. The different kinetic models, pseudo-first-order model (PFO), Elovich model, pseudo-second-order model (PSO) and intraparticle diffusion can be applied to determine the rate as well as the mechanism of the adsorption process. Lagergren proposed the pseudo-first-order model (PFO) in the following equation.

$$\log(q_e - q_t) = \log q_e - \left(\frac{K_1}{2.303}\right)t \tag{10}$$

where q_e (mg/g) is BG (adsorbed amount) by *Pyrus pashia* leaves at equilibrium and k_1 (1/min) is the rate constant for the pseudo-first-order model. The graph of $\ln(q_e - q_t)$ vs. t (Fig. 13) was employed to calculate the k_1 (PFO rate constant). The calculated value of k_1 is presented in Table 4. The PFO model has also been previously applied for the analysis of data [31]. Adsorption kinetics of BG by *Pyrus pashia* leaves was also analyzed by the pseudo-second-order model [Eq. (11)].

$$\frac{t}{q_t} = \frac{1}{k_2 q_e^2} + \left(\frac{1}{q_e}\right)t \tag{11}$$

Table 3
BG loaded *Pyrus pashia* leaves results for the isotherm adsorption model

T (K)	Langmuir constant					Freundlich constant				Temkin constant		
	Q_0 (mg/g)	b (L/mg)	R^2	R_L	SSE	K_F	N	$1/n$	R^2	B	K_t	R^2
303	5.208	3.55	0.99	0.005	67.27	26.42	1.82	0.54	0.98	0.255	1.0815	0.98
313	3.802	5.05	0.97	0.004	87.12	17.06	1.68	0.59	0.97	0.239	0.702	0.98
323	9.174	2.13	0.99	0.007	15.17	55.08	1.81	0.55	0.98	0.238	1.550	0.99

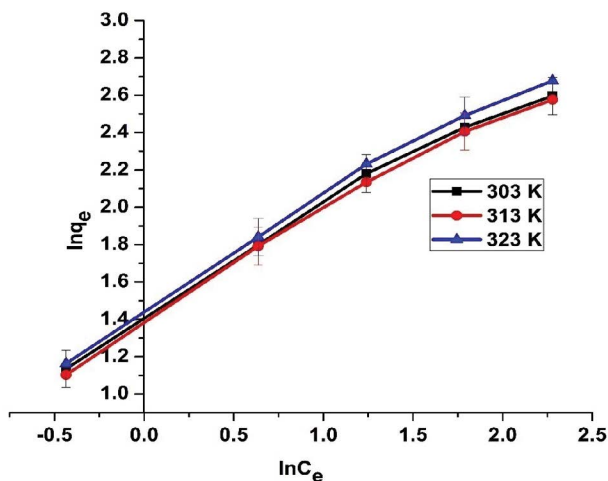


Fig. 11. Freundlich isotherm model results at various temperatures for BG adsorbed *Pyrus pashia* leaves.

The plot of t vs. t/q_t was drawn as shown in Fig. 14 for the calculation of adsorption capacity at equilibrium (q_e) and the constant (k_2) for pseudo-second-order. The values of R^2 (correlation coefficient) ≥ 0.98 of the PSO model were greater than PFO shown in Table 4. The table shows that $q_{e,cal}$ values increased as the initial dye concentration increases. The $q_{e,cal}$ values are best constraints with $q_{e,exp}$ values, for the PSO model [Eq. (11)], where the possibility of a rate-limiting step is afforded by the PSO model which controls adsorption of dye on activated carbon. Similar behavior has been delineated from hydrogen sulfide treated bagasse [41] and *Euphorbia rigida* [40]. The BG removal behavior in the kinetic models suggests that the

Table 4
Results of kinetic studies in BG removal

C_0 (mg/L)	Pseudo-first-order kinetic			Pseudo-second-order kinetic			SSE	Elovich model			Intraparticle diffusion model		
	q_e (mg/g)	k_1 (min^{-1})	R^2	q_e (mg/g)	k_2 ($\times 10^3$ g/(mg min))	R^2		a	b	R^2	K_i (mg/g $\text{min}^{1/2}$)	C	R^2
10	1.407	0.06	0.88	2.07	0.02	0.98	0.44	0.610	0.50	0.92	0.21	0.09	0.97
20	4.470	0.05	0.93	5.98	0.05	0.99	2.28	1.763	1.61	0.99	0.66	0.04	0.97
30	7.247	0.04	0.94	7.24	0.02	0.98	1.00	2.321	2.47	0.98	1.09	0.39	0.96
40	10.33	0.03	0.96	11.62	0.04	0.98	1.66	2.131	3.13	0.96	1.27	1.35	0.93
50	15.55	0.04	0.93	19.23	0.06	0.99	13.54	4.736	5.04	0.98	2.08	0.65	0.98

diffusion mechanism does not account for these models. Elovich model (EM) was also studied for the analysis of experimental data and its equation is shown as:

$$q_t = a + b \ln t \tag{12}$$

The graph of $\ln t$ vs. q_t was employed for the calculation of constants a and b (Fig. 15), which shows a linear relationship [42]. The adsorption kinetics of BG dye on *Pyrus pashia* leaves depending on R^2 values followed the following order PSO > EM > PFO of kinetic models.

3.13. Statistical analysis

The given equation [Eq. (13)] was applied for error analysis, the sum of squared error (SSE).

$$SSE = \sum_{i=1}^n (q_{e,calc} - q_{e,meas})^2 \tag{13}$$

The best matching of experimental data with lower SSE values are shown in Tables 3 and 4.

3.14. Intraparticle diffusion

The intraparticle diffusion was studied by the application of Weber and Morris plots [43] for the investigation of the mechanism of BG adsorption onto *Pyrus pashia* leaves. According to Eq. (14), the adsorption mechanism depicting the diffusion process, the graph of q_t and $t^{1/2}$, should be linear [22] and this model is typically represented as:

$$q_t = K_i t^{1/2} + C \tag{14}$$

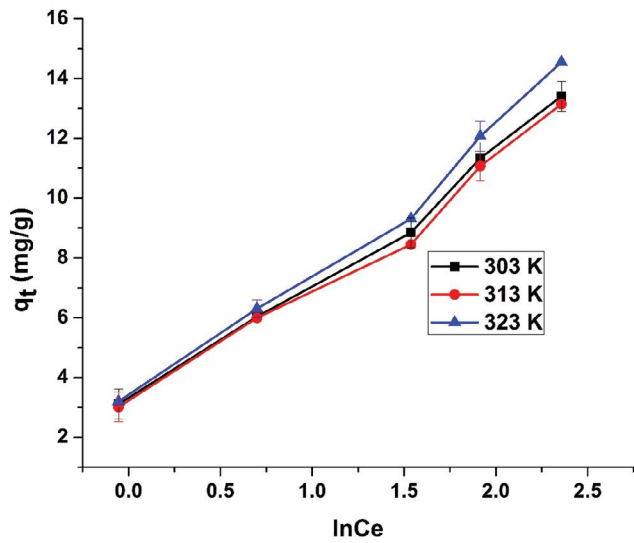


Fig. 12. Temkin isotherm model results at various temperatures for BG adsorbed *Pyrus pashia* leaves.

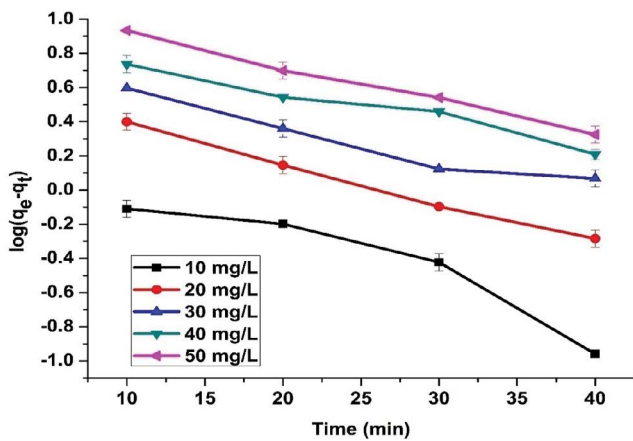


Fig. 13. Pseudo-first-order kinetics for BG adsorbed on *Pyrus pashia* leaves.

where C (mg g^{-1}) denotes the intercept and K_i ($\text{mg g}^{-1} \text{min}^{0.5}$) is the rate constant for intraparticle diffusion. The value of K_i is obtained from the slope of the linear graph between q_t vs. $t^{1/2}$ (Fig. 16). The value of C (Table 4) indicates the boundary layer thickness [44,45]. The deviation from this model shows the difference between the mass transfer rate in the initial and final stages of the adsorption process [46]. The sorption process is affected by two or more steps if the experimental data has multilinear graphs. At the start, the sharper part represented the solute transportation from the bulk solution to the exterior surface of the adsorbent. The next linear part showed the diffusion across the liquid film which is surrounding the adsorbent particle. The third part is due to the diffusion of the particle in the liquid confined in the pore and in the adsorbate along the pore wall. Fig. 16 represented the graph between q_t vs. $t^{1/2}$ for the adsorption of BG onto *Pyrus pashia* leaves for $C_0 = 10, 20, 30, 40,$ and 50 mg/L at 25°C . The graphs were

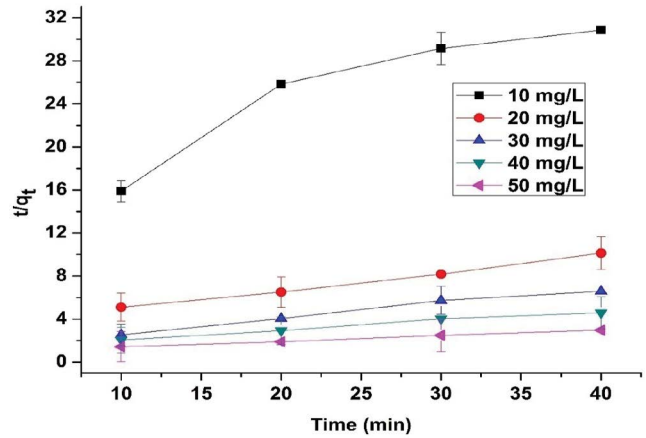


Fig. 14. The kinetics of pseudo-second-order for BG adsorbed *Pyrus pashia* leaves.

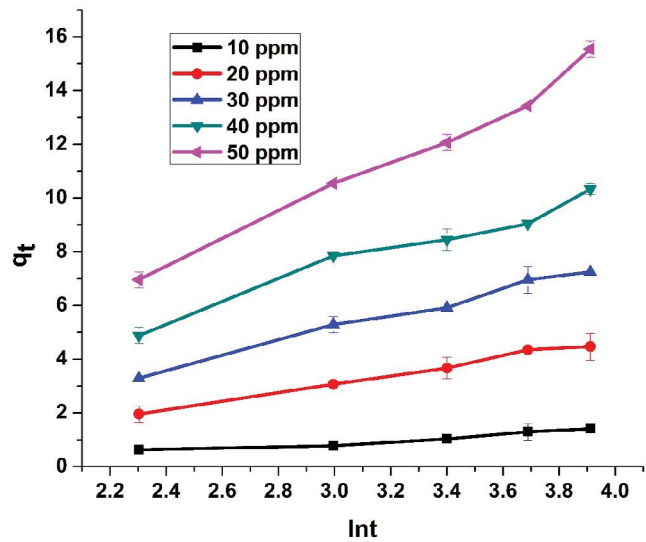


Fig. 15. The Elovich model for BG adsorbed *Pyrus pashia* leaves.

not linear for the entire time range; which indicated that the process of adsorption is controlled by more than one process such as intraparticle diffusion and surface adsorption. The two straight parts or portions were observed for $C_0 = 30, 40,$ and 50 mg/L , the first and second linear portions showing mesopore diffusion and the micropore diffusion, respectively [46]. Whereas one linear part showed combined mesopore diffusion for $C_0 = 20$ and 30 mg/L . Hence in the process of adsorption, the intraparticle BG diffusion in the pores is the rate-controlling step. Comparatively the quantity of dye and the BG driving force for the process of adsorption is less for $C_0 = 10$ and 20 mg/L than $C_0 = 30, 40,$ and 50 mg/L ; hence, shows the mesopore adsorption which is the rate-limiting step. For higher concentrations $C_0 = 30, 40,$ and 50 mg/L , the driving force increases which overcome the resistance for adsorption into micropores; which shows the rate-limiting step for higher concentrations. As the initial concentration of BG increases the K_i values also increase

Table 5
Comparative studies of adsorption capacities and removal efficiencies of adsorbents for BG removal

Adsorbents	q_m (mg/g)	References	Adsorbent	% Removal efficiency	References
Cashew nut shell	5.31	[51]	<i>Salix alba</i>	95.2	[45]
Coarse grinded wheat straw	3.82	[52]	Luffa cylindrical sponge	89.9	[56]
Neem leaf powder	3.67	[53]	Homemade activated carbon	98.2	[57]
Fine grinded wheat straw	2.23	[51]	Acron based adsorbents	93.96	[58]
Chitosan cross-linked (beads)	5.60	[54]	Mixed fungal cultures	83.6	[59]
Coir pith carbon	5.87	[55]	<i>Pyrus pashia</i>	93.35	This study
<i>Ficus palmata</i>	6.89	[44]			
<i>Salix alba</i>	15.89	[45]			
<i>Pyrus pashia</i>	15.55	This study			

(Table 4) which showed improved BG diffusion through meso and micropores at higher concentrations because of greater driving forces [47]. The previous study also revealed similar results for the adsorption of BG on sawdust [48], kaolin [49], and rice husk ash [50].

In Table 5 the comparison of removal efficiency and adsorption capacity with other adsorbents have been narrated. It was observed that the *Pyrus pashia* leaves showing greater removal efficiency than luffa cylindrical sponge, Acron based adsorbents and mixed fungal culture. Moreover, *Pyrus pashia* leaves has greater dye uptake capacity than cashew nut shell, neem leaf powder, fine grinded wheat straw, coir pith carbon and *Salix alba*.

3.15. Desorption

The wastewater treatment process can become more economical due to the spent biosorbent regeneration and recovery of dye. The cost of the process may be reduced and also decrease the process dependence on a continuous supply of adsorbent. For this reason, the desorption of adsorbed dyes and the regeneration of adsorbent for another cycle of the application is necessary. The adsorbate selected should be effective, environment friendly and low-cost. The desorption experiments were also performed for the used adsorbent regeneration process. The regeneration possibility experiments for used *Pyrus pashia* leaves were performed by the application of a number of reagents (distilled water, KCl, NaOH and HCl). Table 6 is showing the results of percentage desorption of BG loaded *Pyrus pashia* leaves with different reagents. The 0.1 M HCl demarcates maximum desorption (32.15%).

4. Conclusion

Pyrus pashia leaves were collected from District Bagh, Village Rairban Azad Jammu and Kashmir territory of Pakistan can be employed as low-cost, efficient and excessively available adsorbent for the brilliant green removal from aqueous solutions. The *Pyrus pashia* leaves powder was characterized by FTIR, SEM, Brunauer–Emmett–Teller and TGA/DSC measurements. The effect of various factors such as initial BG concentration, biosorbent dosage, pH, contact time and temperature were investigated. The percent removal of BG was calculated to be 93.35% at 298 K.

Table 6
Desorption studies of BG loaded *Pyrus pashia* leaves

Desorbing reagents	% Desorption
0.1 M HCl	32.15
0.1 M KCl	3.34
0.1 M NaOH	5.47
Distilled water	2.03

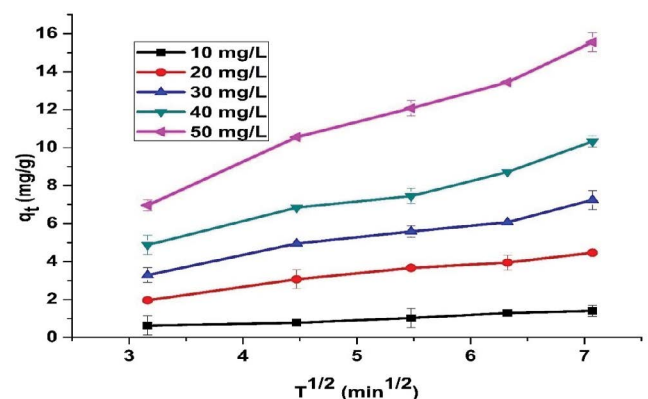


Fig. 16. The results of different dye concentrations for BG removal in the diffusion model.

The obtained results were applied on different isotherm models: Freundlich Temkin, and Langmuir. The Langmuir equation best described the equilibrium isotherms with $R^2 = 0.99$. The equation of the pseudo-second-order model best described the adsorption kinetics. The thermodynamic parameters such as ΔH° , ΔG° and ΔS° were also determined. The adsorbent (*Pyrus pashia* leaves) removed 93% of BG from wastewater which showed that *Pyrus pashia* leaves is a favorable adsorbent for the efficient treatment of wastewater from the textile industry.

References

- [1] R. Ayyappan, A.C. Sophia, K. Swaminathan, S. Sandhya, Removal of Pb(II) from aqueous solution using carbon derived from agricultural wastes, *Process Biochem.*, 40 (2005) 1293–1299.

- [2] S. Dawood, T.K. Sen, Removal of anionic dye Congo red from aqueous solution by raw pine and acid-treated pine cone powder as adsorbent: equilibrium, thermodynamic, kinetics, mechanism and process design, *Water Res.*, 46 (2012) 1933–1946.
- [3] Z.H. Yu, T. Qi, J.K. Qu, L. Wang, J.L. Chu, Removal of Ca(II) and Mg(II) from potassium chromate solution on Amberlite IRC 748 synthetic resin by ion exchange, *J. Hazard. Mater.*, 167 (2009) 406–413.
- [4] K.Z. Elwakeel, M.E. Ahmed, H.M. Samya, Use of beech bivalve shells located at Port Said coast (Egypt) as a green approach for methylene blue removal, *J. Environ. Chem. Eng.*, 5 (2017) 578–587.
- [5] K.Z. Elwakeel, A.A. El-Bindary, A.Z. El-Sanbati, A.R. Hawas, Magnetic alginate beads with high basic dye removal potential and excellent regeneration ability, *Can. J. Chem.*, 95 (2017) 1–28, <https://doi.org/10.1139/cjc-2016-0641>.
- [6] K.Z. Elwakeel, A.A. El-Bindary, A. Ismail, A.M. Morshidy, Sorptive removal of Remazol Brilliant Blue R from aqueous solution by diethylenetriamine functionalized magnetic macro-reticular hybrid material, *RSC Adv.*, 6 (2016) 22395–22410.
- [7] A.K. Meena, G. Mishra, P. Rai, C. Rajagopal, P. Nagar, Removal of heavy metal ions from aqueous solutions using carbon aerogel as an adsorbent, *J. Hazard. Mater.*, 122 (2005) 161–170.
- [8] T.K. Sen, S. Afroze, H.M. Ang, Equilibrium, kinetics and mechanism of removal of methylene blue from aqueous solution by adsorption onto pine cone biomass of *Pinus radiata*, *Water Air Soil Pollut.*, 218 (2011) 499–515.
- [9] N. Jaafarzadeha, Z. Babolib, Z. Noorimotlaghd, S. Silva Martinezf, M. Ahmadi, S. Alavic, S.A. Mirzaee, Efficient adsorption of bisphenol A from aqueous solutions using low-cost activated carbons produced from natural and synthetic carbonaceous materials, *Desal. Water Treat.*, 154 (2019) 177–187.
- [10] Z. Noorimotlagh, R. Darvishi Cheshmeh Soltani, A.R. Khataee, S. Shahriyar, H. Nourmoradi, Adsorption of a textile dye in aqueous phase using mesoporous activated carbon prepared from Iranian milk vetch, *J. Taiwan Inst. Chem. Eng.*, 45 (2014) 1783–1791.
- [11] M. Ghaedi, A. Ansari, M.H. Habibi, A.R. Asghari, Removal of malachite green from aqueous solution by zinc oxide nanoparticle loaded on activated carbon: kinetics and isotherm study, *J. Ind. Eng. Chem.*, 20 (2014) 17–28.
- [12] M. Ghaedi, A.M. Ghaedi, E. Negintaji, A. Ansari, A. Vafaei, M. Rajabi, Random forest model for removal of bromophenol blue using activated carbon obtained from *Astragalus bisulcatus* tree, *J. Ind. Eng. Chem.*, 20 (2014) 1793–1803.
- [13] M. Ghaedi, A. Ansari, F. Bahari, A.M. Ghaedi, A. Vafaei, A hybrid artificial neural network and particle swarm optimization for prediction of removal of hazardous dye brilliant green from aqueous solution using zinc sulfide nanoparticle loaded on activated carbon, *Spectrochim. Acta, Part A*, 137 (2015) 1004–1015.
- [14] V.K. Gupta, Suhas, I. Ali, V.K. Saini, Removal of rhodamine B, fast green, and methylene blue from wastewater using red mud, an aluminum industry waste, *Ind. Eng. Chem. Res.*, 43 (2004) 1740–1747.
- [15] W.T. Tsai, K.J. Hsien, H.C. Hsu, Adsorption of organic compounds from aqueous solution onto the synthesized zeolite, *J. Hazard. Mater.*, 166 (2009) 635–641.
- [16] N.M. Mahmoodi, B. Hayati, M. Arami, C. Lan, Adsorption of textile dyes on pine cone from colored wastewater: kinetics, equilibrium and thermodynamic studies, *Desalination*, 268 (2011) 117–125.
- [17] M. Sciban, M. Klasnja, B. Skrbic, Adsorption of copper ions from water by modified agricultural by-products, *Desalination*, 229 (2008) 170–180.
- [18] R. Sivaraj, C. Namasivayam, K. Kadirvelu, Orange peel as an adsorbent in the removal of acid violet 17, *Water Air Soil Pollut.*, 223 (2001) 5267–5282.
- [19] R. Ahmad, R. Kumar, Adsorption studies of hazardous malachite green onto treated ginger waste, *J. Environ. Manage.*, 91 (2010) 1032–1038.
- [20] P. Saha, Assessment on the removal of methylene blue dye using tamarind fruit shell as biosorbent, *Water Air Soil Pollut.*, 213 (2010) 287–299.
- [21] H.M.F. Freundlich, Over the adsorption in solution, *J. Phys. Chem.*, 57 (1906) 385–470.
- [22] A. Ergene, S. Tan, H. Katurcoglu, Z. Oktem, Biosorption of copper(II) on the *Synechocystis aquatilis*, *Fresenius Environ. Bull.*, 15 (2006) 283–288.
- [23] M.K. Haafiz, S.J. Eichhorn, A. Hassan, M. Jawaid, Isolation and characterization of microcrystalline cellulose from oil palm biomass residue, *Carbohydr. Polym.*, 93 (2013) 628–634.
- [24] M. Poletto, V. Pistor, M. Zeni, A.J. Zattera, Crystalline properties and decomposition kinetics of cellulose fibers in wood pulp obtained by two pulping processes, *Polym. Degrad. Stab.*, 96 (2011) 679–685.
- [25] A.L. Sullivan, R. Ball, Thermal decomposition and combustion chemistry of cellulosic biomass, *Atmos. Environ.*, 47 (2012) 133–141.
- [26] D. Trache, A. Donnot, K. Khimeche, R. Benelmir, N. Brosse, Physico-chemical properties and thermal stability of microcrystalline cellulose isolated from Alfa fibres, *Carbohydr. Polym.*, 104 (2014) 223–230.
- [27] C.P. Azubuike, A.O. Okhamafe, Physicochemical, spectroscopic and thermal properties of microcrystalline cellulose derived from corn cobs, *Int. J. Recycl. Org. Waste Agric.*, 1 (2012) 1–9, <https://doi.org/10.1186/2251-7715-1-9>.
- [28] B. Royer, N.F. Cardoso, E.C. Lima, J.C.P. Vaghetti, N.M. Simon, T. Calvete, R.C. Veses, Applications of Brazilian pine-fruit shell in natural and carbonized forms as adsorbents to removal of methylene blue from aqueous solutions—kinetic and equilibrium study, *J. Hazard. Mater.*, 164 (2009) 1213–1222.
- [29] O. Yunus, Kinetics of adsorption of dyes from aqueous solution using activated carbon prepared from waste apricot, *J. Hazard. Mater.*, 137 (2006) 1719–1728.
- [30] F. Çolak, N. Atar, A. Olgun, Biosorption of acidic dyes from aqueous solution by *Paenibacillus macerans*: kinetic, thermodynamic and equilibrium studies, *Chem. Eng. J.*, 150 (2009) 122–130.
- [31] A. Mahir, C. Sermet, D. Zkan, O.D. Mehmet, Removal of reactive blue 221 and acid blue 62 anionic dyes from aqueous solutions by sepiolite, *Dyes Pigm.*, 65 (2005) 251–259.
- [32] Z. Aksu, S. Tezer, Biosorption of reactive dyes on the green alga *Chlorella vulgaris*, *Process Biochem.*, 40 (2005) 1347–1361.
- [33] N.F.Y. Tam, A.M.Y. Chong, Y.S. Wong, Removal of tributyltin (TBT) by live and dead microalgal cells, *Mar. Pollut. Bull.*, 45 (2002) 362–371.
- [34] C.J. Tien, Biosorption of metal ions by freshwater algae with different surface characteristics, *Process Biochem.*, 38 (2002) 605–613.
- [35] U.J. Kim, S.H. Eom, M. Wada, Thermal decomposition of native cellulose: influence on crystallite size, *Polym. Degrad. Stab.*, 95 (2010) 778–781.
- [36] M. Ghaedi, A. Hassanzadeh, S. Nasir, I.K. Khdan, Multiwalled carbon nanotubes as adsorbents for the kinetic and equilibrium study of the removal of Alizarin red S and Morin, *J. Chem. Eng. Data*, 6 (2011) 2511–2520.
- [37] I. Langmuir, Adsorption of gases on plane surfaces of glass mica platinum, *J. Am. Chem. Soc.*, 40 (1918) 136–403.
- [38] T.W. Weber, R.K. Chakravorti, Pore and solid diffusion models for fixed-bed adsorbents, *AIChE J.*, 20 (1974) 220–228.
- [39] F. Haghseresh, G.Q. Lu, Adsorption characteristics of phenolic compounds onto coal-reject-derived adsorbents, *Energy Fuels*, 12 (1998) 1100–1107.
- [40] A. Mittal, D. Kaur, J. Mittal, Applicability of waste materials—bottom ash and deoiled soya—as adsorbents for the removal and recovery of a hazardous dye, brilliant green, *J. Colloid Interface Sci.*, 326 (2008) 8–17.
- [41] A.Z. Aroguz, J. Gulen, R.H. Evers, Adsorption of methylene blue from aqueous solution on pyrolyzed petrified sediment, *Bioresour. Technol.*, 99 (2008) 1503–1508.
- [42] O.M. Paşka, C. Păcurariu, S.G. Muntean, Kinetic and thermodynamic studies on methylene blue biosorption using corn-husk, *RSC Adv.*, 107 (2014) 62621–62630.

- [43] W.J. Weber, J.C. Morris, Kinetics of adsorption on carbon from solution, *J. Sanitary Eng. Div.*, 89 (1963) 31–59.
- [44] R. Fiaz, M. Hafeez, R. Mahmood, *Ficus palmata* leaves as a low-cost biosorbent for methylene blue: thermodynamic and kinetic studies, *Water Environ. Res.*, 91 (2019) 689–699.
- [45] R. Fiaz, M. Hafeez, R. Mahmood, Removal of brilliant green (BG) from aqueous solution by using low cost biomass *Salix alba* leaves (SAL): thermodynamic and kinetic studies, *J. Water Reuse Desal.*, 10 (2020) 70–81.
- [46] S.G. Muntean, A. Todea, M.E. Rădulescu-Grad, A. Popa, Decontamination of colored wastewater using synthetic sorbent, *Pure Appl. Chem.*, 86 (2014) 1771–1780.
- [47] R. Băbuță, A. Popa, C. Păcurariu, E.S. Dragan, I. Lazau, Adsorption of some phenolic compounds on a new styrene-15% divinylbenzene copolymer functionalized with carboxylic groups volume, *Chem. Bull. Politehnica Univ. Timisoara, ROMANIA, Ser. Chem. Environ. Eng.*, 60 (2015) 1–6.
- [48] V. Garg, R. Gupta, Y.A. Bala, R. Kumar, Dye removal from aqueous solution by adsorption on treated sawdust, *Bioresour. Technol.*, 89 (2003) 121–124.
- [49] B.K. Nandi, A. Goswami, M.K. Purkait, Adsorption characteristics of brilliant green dye on kaolin, *J. Hazard. Mater.*, 161 (2009) 387–395.
- [50] V. Vadivelan, K.V. Kumar, Equilibrium, kinetics, mechanism, and process design for the sorption of methylene blue onto rice husk, *J. Colloid Interface Sci.*, 286 (2005) 90–100.
- [51] P.S. Kumar, R.V. Abhinaya, K.G. Lashmi, V. Arthi, R. Pavithra, V. Sathyaselvabala, S.D. Kirupha, S. Sivanesan, Adsorption of methylene blue dye from aqueous solution by agricultural waste: equilibrium, thermodynamics, kinetics, mechanism and process design, *Colloid J.*, 73 (2011) 651–661, <https://doi.org/10.1134/S1061933X11050061>.
- [52] F.A. Batzias, D.K. Sidiras, E. Schroeder, C. Weber, Simulation of dye adsorption on hydrolyzed wheat straw in batch and fixed-bed systems, *Chem. Eng. J.*, 148 (2009) 459–472.
- [53] K.G. Bhattacharyya, A. Sharma, Kinetics and thermodynamics of Methylene Blue adsorption on Neem (*Azadirachta indica*) leaf powder, *Dyes Pigm.*, 65 (2005) 51–59, <https://doi.org/10.1016/j.dyepig.2004.06.016>.
- [54] I.Y. Kimura, M.C.M. Laranjeira, V.T. Fávere, L. Furlan, The interaction between reactive dye containing vinylsulfone group and chitosan microspheres, *Int. J. Polym. Mater.*, 51 (2002) 759–768, <https://doi.org/10.1080/714975829>.
- [55] D. Kavitha, C. Namasivayam, Experimental and kinetic studies on methylene blue adsorption by coir pith carbon, *Bioresour. Technol.*, 98 (2007) 14–21, <https://doi.org/10.1016/j.biortech.2005.12.008>.
- [56] S.E. Olaseni, N.A. Oladoja, O. Olanrewaju, O.A. Christopher, O.O. Medinat, Adsorption of brilliant green onto luffa cylindrical sponge: equilibrium, kinetics, and thermodynamic studies, *ISRN Phys. Chem.*, 2014 (2014) 743532, <https://doi.org/10.1155/2014/743532>.
- [57] C. Tatiana, C.L. Eder, F.C. Natali, L.P.D. Silvio, S.R. Emerson, Removal of brilliant green dye from aqueous solutions using home made activated carbons, *Clean – Soil Air Water*, 38 (2010) 521–532.
- [58] M. Ghaedi, H. Hossainian, M. Montazerzohori, A. Shokrollahi, F. Shojaiapur, M. Soylak, M.K. Purkait, A novel acron based adsorbent for the removal of brilliant green, *Desalination*, 281 (2011) 226–233.
- [59] P. Wioletta, Z.-G. Ewa, G.-S. Elżbieta, Effectiveness of dyes removal by mixed fungal cultures and toxicity of their metabolites, *Water Air Soil Pollut.*, 224 (2013) 1534, <https://doi.org/10.1007/s11270-013-1534-0>.